Airfoil Aerodynamics in Icing Conditions

M.B. Bragg,* G.M. Gregorek,† and J.D. Lee†
Ohio State University, Columbus, Ohio

Methods of analyzing and experimentally measuring the effect of ice accretion on airfoil sections are presented. Empirical and analytical methods for predicting airfoil performance degradation due to ice are discussed. Ice simulation techniques for aerodynamic testing are presented and compared to data with actual ice accretions. The results show that simulation techniques to imitate the effect of ice on airfoil performance work well in most cases. Comparisons between predicted and measured airfoil performance with ice accretions are presented. For rime ice cases, the predictions compare well with experiment; but for glaze ice, a need for improved methods are seen.

Nomenclature

c	= airfoil chord length
C_d	= airfoil drag coefficient
C_ℓ	= airfoil lift coefficient
C_m	= airfoil moment coefficient
C_p	= pressure coefficient
k	= roughness height
M	= Mach number
Re	= Reynolds number
t_{ice}	= icing time
T_t	= total temperature
α	= airfoil geometric angle of attack
α_{L0}	= zero lift angle of attack
δ_f	= flap deflection
θ	= boundary layer momentum thickness

Introduction

THE accretion of structural ice on aircraft in flight causes a loss in operational efficiency and, more importantly, a reduced safety margin. While deicing and anti-icing systems are available and work well in many applications, they have a high initial cost, add weight to the aircraft, and are expensive to maintain. Therefore, many airfoil surfaces on aircraft are unprotected and designers would like to protect as few surfaces as possible. Therefore, it is important to understand the accretion of ice on unprotected airfoils and the resultant aerodynamic effects.

Early airfoil performance tests were conducted by the NACA in the Lewis Icing Research Tunnel (IRT) in the 1950s. The most complete of these tests was reported by Gray[1] and Gray and von Glahn.[2] Here, well-documented ice accretion and airfoil performance data are presented for an NACA 65A004 airfoil. Lift, drag, and pitching moment changes due to ice accretion were measured with a tunnel balance system. Gray later combined these data and other NACA data as the basis for an empirical equation to predict drag rise due to ice accretion.[3] After this work, little icing research was conducted or published until the current NASA program began in the late 1970s.

The work reported here has been conducted by the authors under NASA sponsorship over the past few years. The purpose of the analysis was to explore the use of currently available airfoil analysis codes to predict airfoil performance due to ice accretion. In many cases, the comparisons were good and, in other cases, areas for further code development were identified. Experimental techniques were developed to test simulated ice shapes on airfoils. These data provide some insight into the effect of ice on airfoil performance and provide data for the analysis. The results presented here are a summary of this work; more detailed descriptions can be found in Refs. 4-10.

Experimental Techniques and Results

While the effect of the weight of ice accreted is usually negligible for fixed wing aircraft, the aerodynamic performance penalty may be severe. Ice accretion changes the gross shape of the airfoil section and adds surface roughness. In most cases, these changes lead to increased drag and decreased lift at constant angles of attack. As a result, the airfoil performance is degraded, as is the efficiency of the total aircraft, propeller, or rotor system. Safety problems may also arise due to the reduced $C_{\ell_{\max}}$ and therefore increased stalling speed. A drastic drag rise may also prevent the aircraft from maintaining level flight.

Experimental testing of airfoils with ice accretions to obtain aerodynamic data is very difficult. In flight, icing conditions are hard to measure and fluctuate greatly as the aircraft passes in and out of the clouds. After ice has been collected, shedding or sublimation often occurs before the shape can be documented and the testing completed. Even if no shedding takes place, instrumenting an airfoil for detailed aerodynamic data acquisition in an icing environment is extremely difficult, especially in flight. In an icing wind tunnel such as NASA's IRT, icing conditions can be well controlled, but again operating instrumentation for detailed measurements is difficult. To avoid these problems, tests with simulated ice shapes are conducted.

To simulate the ice, the ice shape is usually taken from an icing wind tunnel or flight test. Care must be taken to duplicate both the gross shape of the accretion and the character of the surface roughness. For a two-dimensional airfoil test, a two-dimensional ice simulation is usually used, where the cross section of the ice is constant along the span. In this section, simulation techniques are discussed and aerodynamic data are presented.

Received July 22, 1985; revision received Sept. 17, 1985.

*Assistant Professor, Department of Aeronautical and Astronautical Engineering. Member AIAA.

†Professor, Department of Aeronautical and Astronautical Engineering. Member AIAA.

Low-Speed Tests

A section of a general aviation wing was used for this test in the NASA Lewis Icing Research Tunnel.[8] The model was a 1.36 m chord and 2 m span of an NACA 63A415 airfoil section. The ice accretion was conducted at a freestream velocity of 51 m/s, angle of attack of 2.6 deg, liquid water content of 1.5 g/m^3, and a volume median diameter water droplet of 15 μm.[3] The ice shapes and resulting drag rise are shown in Fig. 1. Both the glaze and rime cases are shown, with the only difference being the airstream total temperature, -4 and -26°C, respectively. The drag rise ΔC_d is the increase in drag coefficient above the clean model value. These measurements were taken in the NASA IRT using a wake survey probe. The glaze ice case develops the classical double-horned shape in 15 min and has a much larger drag penalty compared to the more streamlined rime ice.

No lift or pitching moment data are available from the IRT icing tests; these data must come from simulations based on tracings of the ice. Tracings were made by removing a section of the ice accretion using a steam-heated scraper. An airfoil template was then fit over the leading edge and the ice shape traced. From these tracings, simple two-dimensional replicas of the ice shapes could be made. The ice shapes depicted in Fig. 1 are from these tracings.

From these tracings, smooth two-dimensional models of the ice shapes were constructed of mahogany and attached to the airfoil leading edge. Figure 2 shows the simulated rime ice shape on the model in the IRT test section. To simulate the surface roughness of the rime and glaze ice, grit is applied to the surface using a spray adhesive. The model was fitted with external pressure belts for measuring the airfoil surface static pressures. Each ice shape was tapped internally to measure 10 surface pressures. A traversing wake survey probe was also attached to the model in addition to the IRT probe. Data acquisition of the surface pressures and wake data as well as reduction were performed by the Ohio State University (OSU) digital data acquisition and reduction system.[11]

In Fig. 3, the measured drag rise for the simulated rime ice is compared to that of the actual ice. Also shown is the drag rise for the simulated shape without the added surface roughness. The ice simulation appears to be quite good based on the drag values. Note that without roughness the drag rise is greatly reduced, emphasizing the role that the surface roughness plays in the drag of rime ice shapes. For glaze ice shapes, the effect of surface roughness on the drag was found to be small. Here the drag increase is due primarily to flow separation aft of the ice horns and is not significantly affected in most cases by the roughness. For the four cases (two rime and two glaze) tested in this experiment, the simple ice simulation method worked quite well.

For each of the ice simulations, surface pressure and wake data were taken over a range of angles of attack and flap deflections.[9] Thus, for each case, airfoil pressure distributions and integrated lift, drag, and pitching moment data are available. An interesting effect on the airfoil lift due to a rime ice shape accreted at 6.6 deg angle of attack and with no flap deflection is shown in Fig. 4. While in all other cases the ice accretion reduced $C_{\ell_{max}}$, here with no flap deflection the maximum lift is increased slightly. The small streamline ice shape, accreted at high angle of attack, is acting essentially as a leading-edge flap. This had been seen before by NACA researchers. Here, the configuration does have reduced $C_{\ell_{max}}$ for all nonzero flap deflections and has a large drag rise at cruise due to lower surface separation from the ice shape lower horn.

The model was also equipped with a 25% chord, single-slotted fowler flap. Data were taken at flap deflections of 0, 10, 20, and 30 deg on the clean model and with the rime and glaze ice accretions shown in Fig. 1. In Table 1 the lift performance of the airfoil with flap deflection is shown. In some

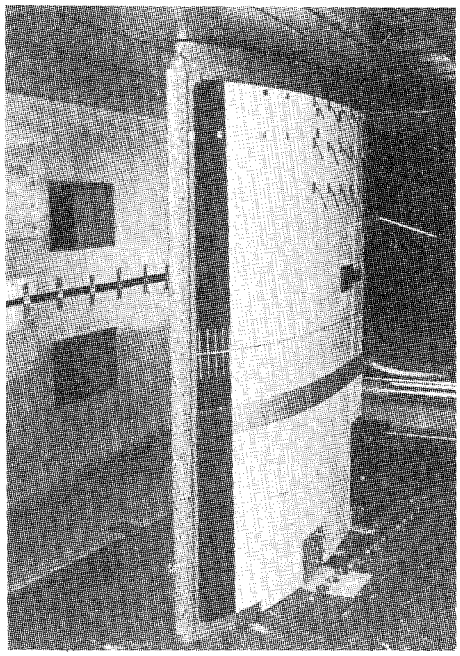

Fig. 2 Instrumented model in IRT with simulated cruise rime ice.

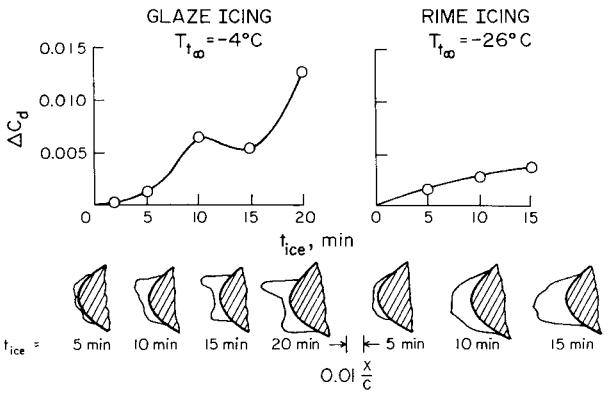

Fig. 1 Comparison of glaze and rime icing for cruise conditions.

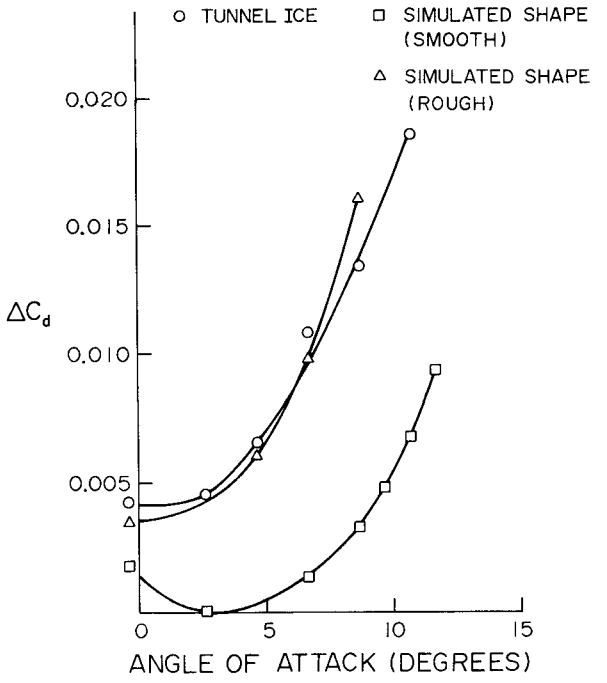

Fig. 3 Effect of natural and simulated cruise rime ice on airfoil drag.

cases α_{L0} is not available, since only data near $C_{\ell_{max}}$ were taken. The two major effects of ice on lift are: a reduction in $C_{\ell_{max}}$ due to premature leading-edge stall and a shift in α_{L0} due to the increased upper surface boundary-layer thickness from the leading-edge roughness. Note that, for this airfoil with these ice accretions, the $C_{\ell_{max}}$ penalty due to the ice is small at zero flap deflection, but is a fairly significant value of approximately 0.3 at flap deflections between 10 and 30 deg.

High-Speed Icing Tests

As part of a helicopter icing flight-test program, ice accretions were documented using several different methods. The purpose of the test was to document ice accretions on rotor blades, which could then be simulated for an aerodynamic wind tunnel test.[10]

The helicopter hovered in the icing cloud the desired time and, immediately after landing, one of the blades was enclosed in a controlled environment for ice shape documentation. The ice shapes were documented at 10 spanwise stations using three different techniques: ice tracings, stereophotography, and silicone molding. The ice tracing technique was similar to that described earlier and the stereophotography method can be found in Ref. 10. The silicone rubber molding technique was based upon work done at NASA Lewis Research Center.[12] A Dow-Corning silicone rubber compound with a hardening catalyst suitable for use at subfreezing temperatures was used. This compound sets up in 2-4 h and, since it was at subzero temperatures, damage to the ice and loss of detail were minimized. After degassing the mixture, it was poured into mold boxes that fit around the ice shape and airfoil leading edge. After about 2 h, the temperature was increased, the mold boxes removed, and the ice still in the molds allowed to melt as the rubber continued to harden. One of the silicone ice molds is shown in Fig. 5. Studying the most forward end, the cross section of the airfoil can be seen along with the impression of the glaze ice shape. Note the excellent detail in the impression of the ice surface roughness in the mold.

The ice shapes from the helicopter were then used to conduct a wind tunnel evaluation of the rotor section aerodynamics. The ice shapes were simulated in two ways. The first method involves casting, from the rubber mold, the ice shape onto a full-scale portion of the blade. This was accomplished using epoxy with a parting compound to minimize damage to the mold. The first casting was made at the model midspan, then others alternately on either side until the 6 in. span mold was cast on the entire blade section. This casting method produced excellent detail in the ice shape.

These shapes were internally tapped as was the airfoil. The second ice simulation involved two-dimensional wooden ice shapes with grit applied to simulate roughness, similar to the method described earlier. Data were taken from the surface pressures and a wake survey probe to determine lift, drag, and moment coefficients.

Full-scale tests of the rotor blade section were conducted in the 65 in. transonic facility of Fluidyne Engineering Corp. using both simulation methods. Scaled simulation was also conducted using the second method in the OSU 6×12 in. transonic airfoil tunnel. In Fig. 6, the drags from the different methods in the Fluidyne tunnel are compared. The two-dimensional wood shape with roughness duplicated the drag rise due to the cast ice shape very well. Unfortunately, no drag data with the actual ice shape is available for comparison. Based on these and other ice accretion tests, the two-dimensional simulation, even in small scale, duplicates the aerodynamic effects of the ice reasonably well.

Airfoil Aerodynamic Analysis

An empirical equation to predict the drag rise due to ice accretion was first formulated by Gray.[3] This equation is based on the data collected by the NACA primarily in the 1950s. Using correlations for ice horn angle and height, the equation is best suited for glaze conditions. While Gray's equation does provide some guidance, the error in predicted drag rise is often quite large.[13] Gray provided no correlation for lift or pitching moment effects.

Brumby[14] has correlated changes in $C_{\ell_{max}}$ due to various types of airfoil surface roughness or protuberances. While not primarily for ice accretions, this work provides some preliminary estimate of $C_{\ell_{max}}$ changes. However, it is very limited in that it contains no Reynolds number effects and little detail of the actual roughness or protuberance shape or density. Certainly, it fails to predict the measured cases of increased $C_{\ell_{max}}$ due to ice accretions. Better methods with less empiricism are needed to accurately predict the aerodynamic effect of ice on airfoils.

Rime Ice

Rime forms at low temperatures where the droplets freeze on impact. These accretions are generally streamlined in shape with a significant portion of the drag rise due to surface roughness and early boundary-layer transition. Bragg[6] formulated a method to analyze airfoils with rime ice based on

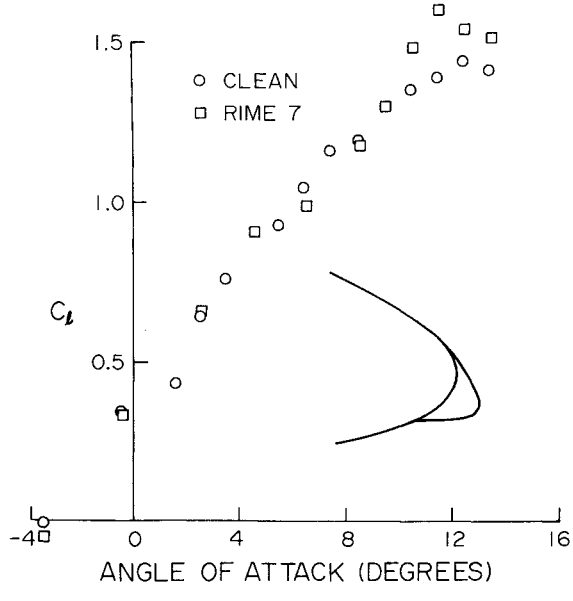

Fig. 4 Lift performance of an airfoil with rime ice accreted at an angle of attack of 6.6 deg.

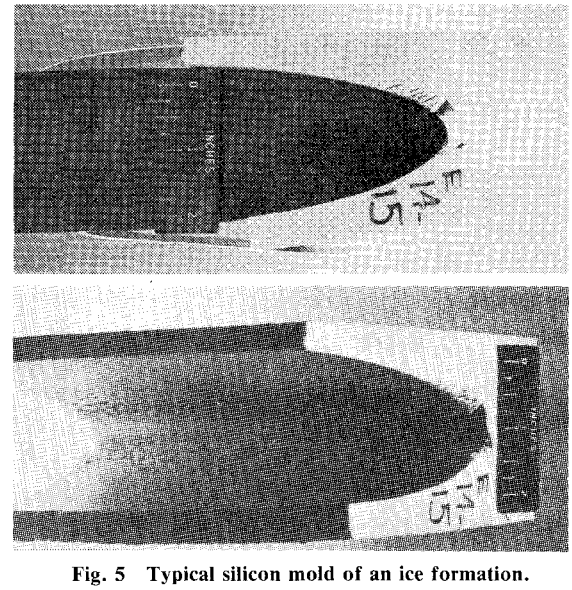

Fig. 5 Typical silicon mold of an ice formation.

existing airfoil analysis computer codes and a simple drag correlation. The method assumes that changes in C_ℓ and C_m can be found by analyzing the airfoil with a smooth ice shape and that C_d can be predicted using an empirical ΔC_d relation.

The airfoil with and without the smooth ice shape is first analyzed using the code of Eppler and Somers.[15] Their simple $C_{\ell_{max}}$ scheme provides a reasonable estimate for $C_{\ell_{max}}$ if the ice shape causes a leading-edge stall. The airfoil analysis code of Smetana et al.[16] includes the boundary-layer displacement effects by iterating on the airfoil plus displacement thickness. By forcing an early transition due to the rime ice roughness, the thickening boundary layer causes a reduction in lift by reducing the angle of attack for zero lift. This also improves the calculation of the pitching moment. Therefore, by combining the results of the two airfoil analysis codes, the lift and pitching moment performance of the airfoil with rime ice can be estimated.

In Fig. 7, a prediction by this method is compared to the measured lift performance of an NACA 65A413 airfoil with simulated rime ice. The comparison is quite good, although the $C_{\ell_{max}}$ with ice was somewhat underpredicted. The shift in the angle of attack for zero lift is accurately predicted. A typical drag prediction is shown in Fig. 8 for the same NACA 65A413 airfoil with simulated rime ice. The current drag correlation includes the effect of surface roughness, rime ice cross-sectional area, and airfoil type only.[4] Comparisons between this method and the measured drag values are acceptable, but the iced airfoil drag is overpredicted. The prediction using Gray's equation[3] compares well at the iced C_ℓ, approximately 0.4, but greatly overpredicts the drag at all other conditions.

To attempt to remove some of the empiricism, a computer program has been developed to model surface roughness and trailing-edge separation. The code is a modified version of the CLMAX program by Dvorak.[17] In this program, the wake region resulting from turbulent boundary-layer separation is modeled using a free vortex sheet of constant strength. A sheet of equal but opposite strength is shed into the wake from the lower surface. An iterative procedure is used to converge on a flowfield solution. An inner iteration loop calculates the wake shape, while the outer iteration recalculates the boundary-layer characteristics and separation point. The potential flow solution is obtained using a panel method with vortex panels. Separation and other boundary-layer characteristics are calculated using a momentum integral method.

Since surface roughness is present for airfoils with ice, the program was modified to activate the rough turbulent boundary-layer method of Dvorak.[18] This is a momentum integral method that includes the effect of roughness in the transitional or fully rough regime with or without a pressure gradient. Since much of the roughness occurs in the laminar boundary layer near the leading edge, a simple modification was made in the laminar boundary-layer routine.[6] After determining the boundary-layer velocity distribution, integration over the roughness height k/c yields the element form drag. A drag coefficient of 0.5 was assumed. Using the known roughness density, the total increment in drag over a boundary-layer step $d(S/c)$ can be determined. This value of ΔC_d was then included into the boundary-layer calculation by incrementing the momentum thickness θ using the Squire-Young law.

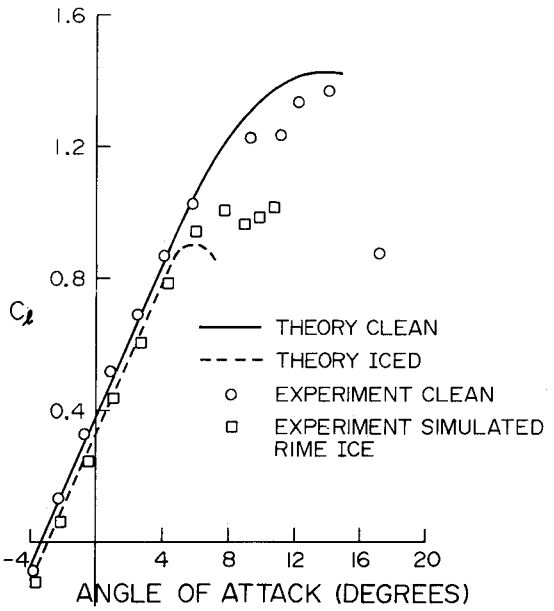

Fig. 7 Measured and predicted lift of an NACA 65A413 airfoil clean and with rime ice.

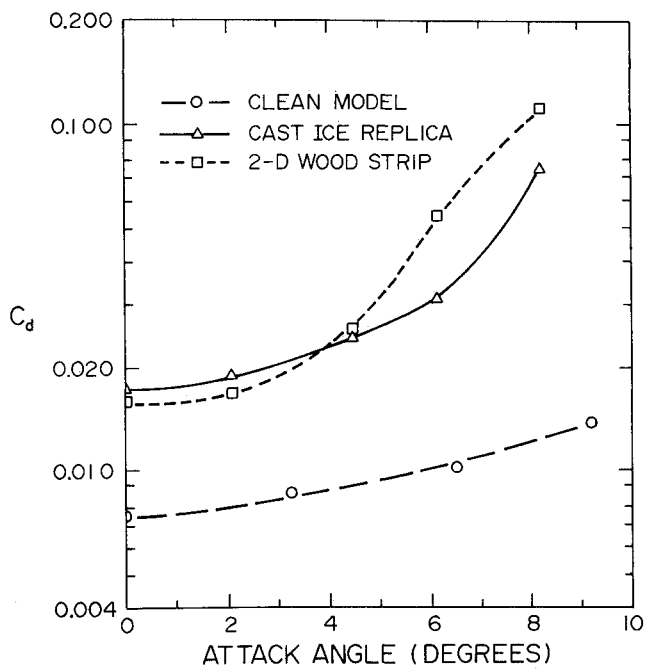

Fig. 6 NACA 0012 rotor airfoil drag—clean and with simulated ice.

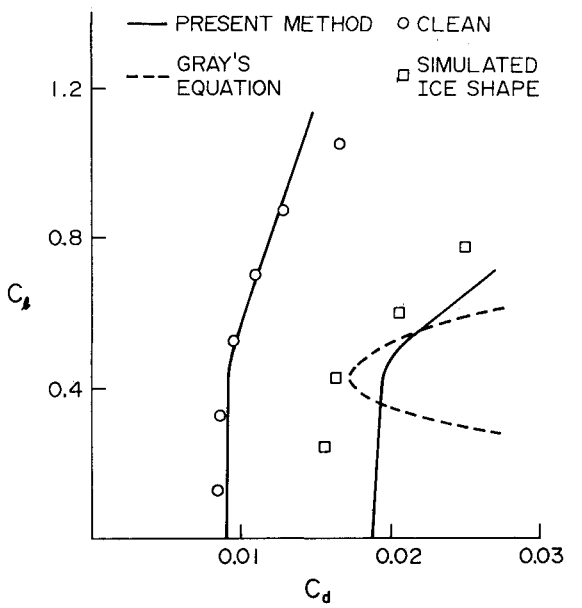

Fig. 8 Measured and predicted drag polars for an NACA 65A413 airfoil clean and with rime ice.

Table 1 Airfoil performance degradation with simulated ice

	$\delta_f = 0$ deg			$\delta_f = 10$ deg			$\delta_f = 20$ deg			$\delta_f = 30$ deg		
Parameter	Clean	Rime	Glaze	Clean	Rime	Glaze	Clean	Rime	Glaze	Clean	Rime	Glaze
$C_{\ell_{max}}$	1.4	1.4	1.3	1.8	1.5	1.4	2.0	1.75	1.7	2.2	1.95	2.0
α_{stall}	12.5	12.5	10.3	14.0	10.5	10.5	12.5	8.5	9.5	11.5	6.5	7.5
α_{L0}	−3.4	−2.6	−3.0	−6.4	−5.8	−5.9	−10.0	—	—	−13.2	−10.0	−12.0

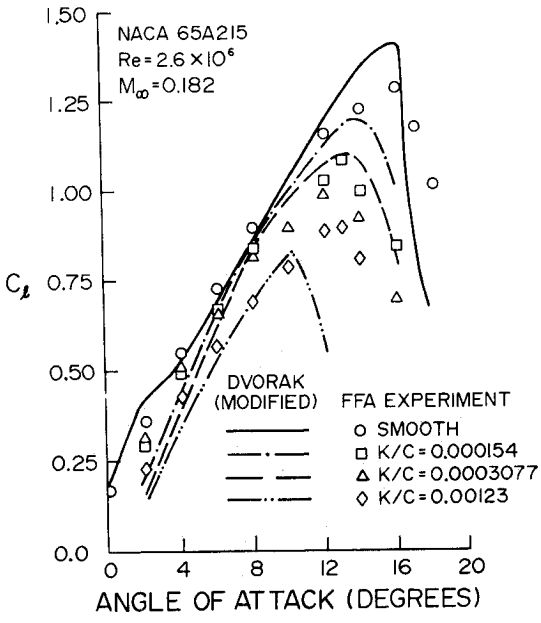

Fig. 9 Comparison of theory to experiment for the lift performance of the NACA 65A215 airfoil with various roughness levels.

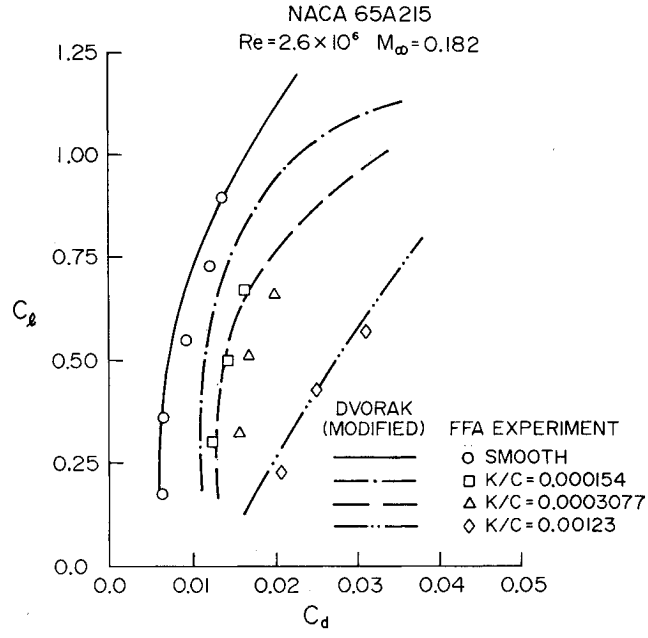

Fig. 10 Theory compared to experiment for the drag of an NACA 65A215 airfoil with various roughness levels.

Implementing this method requires that the roughness height, density, and area covered be input to the computer code. The rough turbulent method was written based on two-dimensional roughness data, but with some information on its use with sand grain roughness. Actual surface roughness is, however, three-dimensional, so to correct for this, the equivalent sand grain roughness is used.

This computer program is compared to experiment for an airfoil with distributed surface roughness in Figs. 9 and 10. In Fig. 9, the lift performance of an NACA 65A215 airfoil for three heights of distributed surface roughness is shown. In the experiment[19] as well as the theory, the roughness covers the entire upper surface and the lower surface from the leading edge to $x/c = 0.15$. While $C_{\ell_{max}}$ is overpredicted in most cases, the reduction in $C_{\ell_{max}}$ with roughness is predicted quite well for all but the largest roughness size. The stall angles are also determined. Although the theory overpredicts $C_{\ell_{max}}$ on the clean airfoil compared to these data, it compares quite well to that measured by the NACA on a similar airfoil.[20]

The theoretical and experimental drag polars for the same airfoil and roughness levels are shown in Fig. 10. The general trend and magnitude of the drag increments are quite good. The clean airfoil drag and that with the largest roughness match experiment very well. The code is an excellent tool to determine drag rise due to roughness, but does have some limitations. In cases where the roughness is three-dimensional, but not sand grain, determining the proper equivalent sand grain roughness is very difficult. Using the correct roughness height is critical if the performance degradation is to be accurately determined. Also, the iterative method sometimes fails to converge. This happens if the airfoil has a trailing-edge separation, then stalls from near the leading edge. The iterative scheme oscillates from a leading-edge to trailing-edge stall. When these difficulties can be avoided, the program yields good results.

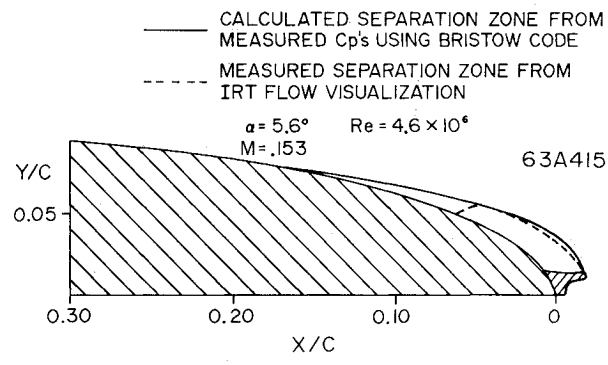

Fig. 11 Predicted bubble geometry using measured surface pressures for the cruise glaze ice shape.

Glaze Ice

Glaze ice accretions occur at temperatures near freezing, where the water droplets run back on the surface before freezing. While rime ice shapes are fairly streamlined, glaze ice accretions usually present a drastic change in the airfoil shape. This results in sometimes large regions of flow separation aft of the ice horns. As a result of the separation, the airfoil experiences a severe drag rise, reduction in $C_{\ell_{max}}$, and some change in pitching moment. At the present time, no analytical

methods are available to predict this separation and its effect on the airfoil. Before such a method can be developed, experimental data must be gathered on which to validate and test these new methods.

Oil flow experiments have been conducted to determine the size of the separated zone aft of a glaze ice horn. A splitter plate carefully aligned with the flow was used to help visualize the time-averaged velocities.[7] The size of the separation zone can be estimated by following a streamline back from the separation at the tip of the horn to the reattachment point, behind which the oil moves back parallel to the surface. Oil flow photographic studies have been conducted for two different glaze ice shapes on the NACA 63A415 airfoil using simulated ice shapes and tested in the NASA Lewis Research Center's IRT.

While no viscous modeling of the flowfield about an airfoil with glaze ice has been done by the authors, some initial potential flow studies have.[7] Here many of the popular airfoil analysis and potential flow codes were evaluated as to their performance on an airfoil with glaze ice. One of the most promising was the potential flow code of Bristow.[21] In addition to operating in the usual analysis mode, this code has a design or mixed boundary condition option in which velocities are input over a region of the airfoil and the corresponding geometry is predicted.

Using the design mode and measured surface pressures in the separated zone, the separation bubble geometry can be estimated. In Fig. 11, such a prediction is shown compared to the measured separation zone from oil flow studies. Shown is the upper surface leading edge of an NACA 63A415 airfoil with a simulated ice shape. The measured and predicted bubbles are very similar for the first 5% chord. Then, however, the oil flow showed reattachment, while the predicted bubble extends back to almost 20% chord. This is not unexpected, since surface velocities defining the design region were input back to 20% chord and the theory should predict the airfoil plus displacement thickness in unseparated regions. Several comparisons have been completed and the results are encouraging.

Comparisons have also been made by calculating the potential flow about the airfoil with glaze ice and adding to the airfoil geometry the geometry of the measured separation streamline. Using this equivalent body, the potential flow codes predict pressures very similar to the measured values in the separated zone. While these potential flow methods cannot, of course, predict the separation bubble a priori, they do provide some insight into the problem.

Summary

The experimental measurement of the aerodynamic effect of ice on airfoils is very difficult due to the icing environment. Therefore, it is usually advantageous to test airfoils with simulated ice shapes. Two ice simulation methods have been discussed. Simple two-dimensional shapes with simulated surface roughness seem to accurately simulate the aerodynamic penalties due to ice in most cases. These results are compared to actual iced airfoil data and to a more sophisticated simulation method. Aerodynamic penalties have been obtained for several cases and are discussed.

Airfoils usually suffer increased drag, reduced lift, and pitching moment change due to ice accretion. Methods for predicting these changes, which include various degrees of empiricism, were discussed. For rime ice accretions, these methods have been fairly successful where the predictions are based on existing airfoil analysis codes with some empirical correction. A single computer code to analyze rime-iced airfoils is presented. Glaze ice accretions are more difficult to analyze due to the large regions of separated flow. Oil flow visualization has been used to view the separated zones. Results from inviscid models based on the measured separation streamlines and surface pressures have been encouraging.

Acknowledgments

This work was supported in part by the NASA Lewis Research Center. The authors would like to thank Dr. R. J. Shaw of NASA Lewis for his many contributions to this research.

References

[1]Gray, V.H., "Correlations Among Ice Measurements, Impingement Rates, Icing Conditions, and Drag Coefficients for Unswept NACA 65A004 Airfoil," NACA TN 4151, Feb. 1958.

[2]Gray, V.H. and von Glahn, U.H., "Aerodynamic Effects Caused by Icing of an Unswept NACA 65A004 Airfoil," NACA TN 4155, 1957.

[3]Gray, V.H., "Prediction of Aerodynamic Penalties Caused by Ice Formations on Various Airfoils," NASA TN D-2166, 1964.

[4]Bragg, M.B., "Rime Ice Accretion and Its Effect on Airfoil Performance," Ph.D. Dissertation, Ohio State University, Columbus, 1981 (also NASA CR 165599, 1982).

[5]Bragg, M.B. and Gregorek, G.M., "Aerodynamic Characteristics of Airfoils with Ice Accretions," AIAA Paper 82-0282, Jan. 1982.

[6]Bragg, M.B. "Predicting Airfoil Performance with Rime and Glaze Ice Accretions," AIAA Paper 84-0106, Jan. 1984.

[7]Zaguli, R.J., "Potential Flow Analysis of Glaze Ice Accretions on an Airfoil," M.S. Thesis, Ohio State University, Columbus, 1983.

[8]Bragg, M.B., Gregorek, G.M., and Shaw, R.J., "Wind Tunnel Investigation of Airfoil Performance Degradation Due to Icing," AIAA Paper 82-0582, March 1982.

[9]Zaguli, R.J., Bragg, M.B., and Gregorek, G.M., "Results of an Experimental Program Investigating the Effects of Simulated Ice on the Performance of the NACA 63A415 Airfoil with Flap," NASA CR 168288, Jan. 1984.

[10]Lee, J.D., "Aerodynamic Evaluation of a Helicopter Rotor Blade with Ice Accretion in Hover," AIAA Paper 84-0608, March 1984.

[11]Freuler, R.J. and Hoffmann, M.J., "Experiences with an Airborne Digital Computer System for General Aviation Flight Testing," AIAA Paper 79-1834, Aug. 1979.

[12]Richter, G.P., Private communication, NASA Lewis Research Center, Cleveland, OH, 1984.

[13]Shaw, R.J., Sotos, R.G., and Solano, F.R., "An Experimental Study of Airfoil Icing Characteristics," NASA TM 82790, Jan. 1982.

[14]Brumby, R.E., "Wing Surface Roughness, Cause and Effect," *DC Flight Approach*, Douglas Aircraft Co., Long Beach, CA, Jan. 1979, p. 207.

[15]Eppler, R. and Somers, D.M., "A Computer Program for the Design and Analysis of Low-Speed Airfoils," NASA TM 80210, Aug. 1980.

[16]Smetana, F.O., Summey, D.C., Smith, N.S., and Carden, R.K., "Light Aircraft Lift, Drag, and Moment Prediction—A Review and Analysis," NASA CR-2523, May 1975.

[17]Dvorak, F., "CLMAX Program Description," AMI Rept. 7905, Contract NASI-15729, NASA Langley Research Center, 1979.

[18]Dvorak, F.A., "Calculation of Turbulent Boundary Layers on Rough Surfaces in Pressure Gradient," *AIAA Journal*, Vol. 7, Sept. 1969, pp. 1752-1759.

[19]Ljungstrom, B., "Wind Tunnel Investigations of Simulated Hoar Frost on a 2-Dimensional Wing Section with and without High Lift Devices," Aeronautical Research Institute of Sweden, FFA, Rept. AU-902, 1972.

[20]Abbott, I.H. and von Doenhoff, A.S., *Theory of Wing Sections*, Dover Publications, New York, 1959.

[21]Bristow, D.R., "Multi-Element Airfoil Inviscid Analysis and Design Program (Version 1): User Instructions," McDonnell Aircraft Co., St. Louis, MO, Dec. 1980.